Electronic Supplementary Material (ESI) for ChemComm.

Electronic Supplementary Information

Photo-uncaging a Ru(II) Intercalator via Photodecomposition of a Bridged Mn(I) PhotoCORM

Rachael N. Pickens*, Grace L. Judd, Jessica K. White

Department of Chemistry and Biochemistry, Ohio University, Athens, OH 45701, USA

Table of Contents

1 **Materials and Reagents**. 3

2 Synthesis of $[(bpy)_2Ru(tpphz)Mn(CO)_3Br](PF_6)_2$ (RuMn-Br). 4

3 Synthesis of $[(bpy)_2Ru(tpphz)Mn(CO)_3(CH_3CN)](PF_6)_3$. 4

4 Instrumentation 5

^{1}H NMR spectroscopy. 5

Elemental analysis. 5

Mass spectrometry. 5

Fourier transform infrared spectroscopy (FT-IR). 5

Electronic absorption spectroscopy. 5

Fluorescence Spectroscopy 5

5 DNA relative viscosity. 6

6 Quantum yield of ligand exchange 6

Figure S 1. Synthetic scheme for the preparation of **RuMn-Br** and **RuMn-CH_3CN**. 7

7 List of Figures 7

Figure S 2. HR-MS of **RuMn-Br** in CH_3CN and simulated spectrum of [RuMn-Br -2(PF_6)]$^{2+}$. 8

Figure S 3. HR-MS of **RuMn-Br** photoproduct in CH_3CN. 8

Figure S 4. HR-MS **RuMn-CH_3CN** in CH_3CN and simulated spectrum of [RuMn-CH_3CN – 2(PF_6)]$^{2+}$ and [RuMn-CH_3CN -3(PF_6)]$^{3+}$. 9

Figure S 5. HS DNA Relative Viscosity $[(bpy)_2Ru(tpphz)Ru(bpy)_2]^{4+}$ (●) and $[Ru(bpy)_3]^{2+}$ (●). 10

Figure S 6. ^{1}H NMR 5.0 mM in CD_3CN of **Ru(tpphz)** (black), **RuMn-Br** (red), and **RuMn-CH_3CN** (blue). 10

Figure S 7. ^{1}H NMR **RuMn-CH_3CN** in CD_3CN. 11

Figure S 8. ^{1}H NMR **RuMn-Br** in CD_3CN. 11

Figure S 9. ^{1}H NMR **Ru(tpphz)** in CD_3CN are varied concentrations. 12

Figure S 10. ^{1}H NMR **RuMn-Br** 5.0 mM (bottom), 2.5 mM (top) in CD_3CN. 12

Figure S 11. Dark Controls, initial (solid black) and 18 h (red dash), in rt water for **RuMn-CH_3CN** (A) and **RuMn-Br** (B). 13

Figure S 12. Dark Controls, initial (solid black) and 18 h (red dash), in rt 5 mM Tris, 50 mM NaCl buffer for **RuMn-CH_3CN** (A) and **RuMn-Br** (B). 13

Figure S 13. Dark Controls, initial (solid black) and 1 h (red dash), in rt CH_3CN for **RuMn-CH_3CN** (A) and **RuMn-Br** (B). 13

Figure S 14. FTIR dark control of **RuMn-Br** (A) and **RuMn-CH_3CN** (B) in rt CH_3CN 0 h (black) and 1 h (red dash). 14

Figure S 15. FTIR spectra for **RuMn-Br** (black) and **RuMn-CH_3CN** (red) in rt CH_3CN (1 mM) in the dark. 14

Figure S 16. FTIR absorbance values versus irradiation time of **RuMn-Br** with wavenumbers of initial complex (blue), the first observable intermediate (red), and second observable intermediate (black) (A) Initial irradiation times (B). 15

Figure S 17. FTIR absorbance values versus irradiation time of **RuMn-CH_3CN** with wavenumbers of initial complex (blue), and the first observable intermediate (black) (A) Initial irradiation times (B). 15

Figure S 18. Absorbance measurements of **RuMn-Br** 470 nm photolysis in rt CH_3CN 0 - 15 min (A) Limited spectral view of 470 nm photolysis of **RuMn-Br** in rt CH_3CN with inset showing overlay of **RuMn-Br** photoproduct with **Ru(tpphz)** in CH_3CN (B). 16

Figure S 19. Absorbance measurements of **RuMn-CH_3CN** 470 nm photolysis in rt CH_3CN 0 - 30 min (A) Limited spectral view of 470 nm photolysis of **RuMn-CH_3CN** in rt CH_3CN with inset showing overlay of **RuMn-CH_3CN** photoproduct with **Ru(tpphz)** in CH_3CN (B). 16
Figure S 20. Absorbance measurements of **RuMn-CH_3CN** 470 nm photolysis in rt 5 mM Tris 50 mM NaCl buffer 0 - 40 min (A) Limited spectral view of 470 nm photolysis of **RuMn-CH_3CN** in rt 5 mM Tris 50 mM NaCl buffer with inset showing overlay of **RuMn-CH_3CN** photoproduct with **Ru(tpphz)** in 5 mM Tris 50 mM NaCl buffer (B). 16
Figure S 21. FTIR absorbance values versus irradiation time of **RuMn-Br** in degassed CH_3CN (A-C) aerated CH_3CN (D-F) with wavenumbers of initial complex (blue), the first observable intermediate (red), and second observable intermediate (black) (B and E) Initial irradiation times (C and F). 17
Figure S 22. Emission spectra of **Ru(tpphz)** (A) **RuMn-Br** photoproduct (B) and **RuMn-CH_3CN** photoproduct (C) 7.5 μM in buffer (5 mM Tris, 50 mM NaCl, pH= 7.5) at room temperature with increasing [CT-DNA] up to 80 μM. A plot of increasing emission intensity at 628 nm as a function of increasing [CT-DNA] for **Ru(tpphz)** (D) **RuMn-Br** photoproduct (E) and **RuMn-CH_3CN** photoproduct (F). 18
8 References 18

1 Materials and Reagents.

All reagents were purchased from commercial sources and used as received. Acetonitrile, diethyl ether, hexanes, methanol, and dichloromethane all ACS grade were purchased from Fisher Scientific. Mass grade Acetonitrile was purchased from Fisher Scientific. Acetonitrile-d3 was purchased from Cambridge Isotope Laboratories. Ruthenium(III) chloride hydrate was purchased from Oakwood Chemical. 2,2'-bipyridine, silver trifluoromethanesulfonate, and sodium hydroxide was purchased from Acros Organics. 5,6-diamino-1,10-phenanthroline was purchased from AmBeed. 1,10-phenanthroline-5,6-dione and potassium hexafluorophosphate were purchased from TCI. Bromopentacarbonylmanganese(I) was purchased from Strem Chemicals. Tetrabutylammonium hexafluorophosphate (98%) was purchased from Alfa Aesar and was recrystallized using ethanol prior to electrochemical analysis. Ferrocene (98%) was purchased from Sigma Aldrich and purified through sublimation prior to electrochemical analysis. Amberlite® IRA-410 chloride form anion exchange resin was purchased from Sigma Aldrich. Tris(hydroxymethyl)aminomethane (Trizma Base) was purchased from Sigma Aldrich. Herring Sperm and calf thymus DNA were purchased from Invitorgen. Sodium Chloride was purchased from Fisher Chemical. Sodium hydroxide (98%, extra pure pellets) was purchased from Acros Organics. $[Ru(bpy)_2(tpphz)](PF6)_2$ was synthesized according to previously reported methods.[1] Solubility of tpphz prevented the synthesis of $Mn(tpphz)(CO)_3Br$ using our previously reported protocols.

2 Synthesis of $[(bpy)_2Ru(tpphz)Mn(CO)_3Br](PF_6)_2$ (RuMn-Br).

To a 100 mL round bottom flask, $[Ru(bpy)_2(tpphz)](PF_6)_2$ (54.9 mg, 0.051 mmol, 1 equiv.) was added with 15 mL CH_2Cl_2. The flask was attached to a condenser and the system was sparged with Argon for 15 min. Excess $Mn(CO)_5Br$ (28.3 mg, 0.103 mmol, 2.0 equiv.) was then added to the solution under positive Argon pressure while in the dark. The reaction mixture was then covered in aluminum foil and heated at reflux for 3 h under an Argon atmosphere. The reaction mixture was then cooled to room temperature, added to diethyl ether to precipitate the product and stirred for 15 minutes. The solid was collected on a fine glass frit and washed with diethyl ether (3 × 15 mL) to remove excess $Mn(CO)_5Br$ and dried under vacuum. Yield: 61.8 mg (0.047 mmol, 93%) ^{1}H NMR (500 MHz); ∂ 10.02 (2 H, m), 9.95 (2H, d), 9.78 (2H, d), 8.57 (2H, d), 8.53 (2H, d), 8.28 (2H, m), 8.23 (2H, m), 8.14 (2H, td), 8.01 (4H, m), 7.87 (2H, m), 7.76 (1H, d) , 7.72 (1H, d), 7.48 (2H, m), 7.25 (2H, m) (HR-ESI(+)-MS (CH_3CN): $[M\text{-}2(PF_6)]^{2+}$, *m/z* = 507.99776 (calc *m/z* = 507.99711) Elemental analysis calculated for RuMn-Br +0.5 H_2O +0.5 CH_2Cl_2 : 42.01% C, 2.23% H, 10.31% N. Found 41.88% C, 2.21% H, 10.28% N.

3 Synthesis of $[(bpy)_2Ru(tpphz)Mn(CO)_3(CH_3CN)](PF_6)_3$.

Ru(tpphz)Mn(Br) (36.5 mg, 0.0279 mmol, 1 equiv.) was added to a 50 mL round bottom flask in the dark. To the same flask, $Ag(PF_6)$ (14.1 mg, 0.0558 mmol, 2 equiv.) was added with CH_3CN (10 mL) in the dark. The sample was then reacted overnight under Argon and filtered through a celite pad in a glass frit and washed with CH_3CN (3 × 15 mL) to filter out AgBr. The filtrate was protected from the light, concentrated under vacuum, and then precipitated in diethyl ether. The solid was collected with a fine glass frit. Yield: 30.8 mg (0.022 mmol, 78%) ^{1}H NMR (500 MHz); ∂ 10.14 (2H, m), 9.97 (2H, d), 9.68 (2H, d), 8.58 (2H, d), 8.54 (2H, d), 8.31 (4H, m), 8.14 (2H, m), 8.02 (4H, m), 7.88 (2H, m), 7.76 (1H, d) , 7.73 (1H, d), 7.49 (2H, m), 7.26 (2H, m) HR-ESI(+)-MS (CH_3CN): $[M\text{-}3(PF_6)]^{3+}$, *m/z* = 326.03436 (calc *m/z* = 326.03396) $[M\text{-}2(PF_6)]^{2+}$, *m/z* = 561.53608 (calc *m/z* = 5561.53331) Elemental analysis calculated for RuMn-CH_3CN +1 H_2O : 41.13% C, 2.32% H, 10.77% N. Found 40.69% C, 2.30% H, 10.83% N.

4 Instrumentation

^{1}H NMR spectroscopy.

^{1}H NMR spectra were collected using a Bruker Ascend 500 MHz spectrometer at 298 K. CD_3CN was used as the solvent, and chemical shifts were referenced to the residual solvent peak for acetonitrile (δ = 1.94 ppm).

Elemental analysis.

Elemental analysis (C, H, N) was performed by Atlantic Microlabs, Inc. (Norcross, GA). Samples were protected from light to prevent photodecomposition prior to analysis.

Mass spectrometry.

HR-ESI(+)-MS spectra were collected using a Thermo Fisher Scientific Q Exactive Plus hybrid quadrupole – Orbitrap mass spectrometer in the positive ion mode. A solution containing 1-10 μM Ru(tpphz)Mn in mass grade CH_3CN was infused directly into the ESI source for ionization. The injection flow rate was 10 μL min^{-1} and the applied potential for ionization was 2.0 kV.

Fourier transform infrared spectroscopy (FT-IR).

FTIR spectra were collected with a Shimadzu IRAffinity-1S Fourier Transform Infrared Spectrophotometer in a CaF_2 liquid IR cell. Samples (1 mM in CH_3CN) were prepared in the dark, irradiated with 470 nm light using in-house built red LEDs purchased from Luxeon Star LEDs (Quadica Developments, Inc., Lethbridge, Alberta, Canada), and IR spectra were measured at time intervals until no further spectral changes were observed. For degassed experiments, the sample in the IR cell was carefully bubbled with nitrogen for 10 minutes and immediately capped.

Electronic absorption spectroscopy.

Absorption spectra were recorded using an Agilent Cary 8454 Diode Array UV-Visible Spectrophotometer (1 nm resolution, 0.5 s integration time). Measurements were obtained in a 1 × 1 cm quartz cuvette at 25 °C. Extinction coefficient measurements were performed in triplicate in the dark. For photolysis experiments, CH_3CN and H_2O solutions were prepared in the dark, irradiated with 470 nm light (as described above), and the spectra were measured at time intervals until no further spectral changes were observed.

Fluorescence Spectroscopy

Emission experiments were performed using a Horiba Scientific Fluoromax-4C system equipped with a 150 W Xe arc lamp, Czerny-Turner excitation (1200 g/mm grating blazed at 330 nm) and emission (1200 g/mm grating blazed at 500 nm) monochromators, and a red-sensitive R928 PMT detector. A procedure was performed similar to a previously reported experiment (JACS, 2005, 127, 10796-10796). Buffer solutions (5 mM tris, 50 mM NaCl, pH= 7.5) containing RuMn-Br and

RuMn-CH_3CN were irradiated with 470 nm light until no further changes in absorbance we observed, excited at 450 nm, and emission was monitored from 500-800 nm. An aliquot of calf thymus DCN (CT-DNA) was added and an increase in emission intensity was monitored as more CT-DNA was added.

5 DNA relative viscosity.

A 500 µL sample of Herring Sperm (HS) DNA (0.5 mM) was prepared in 5 mM Tris, 50 mM NaCl, pH = 7.5 buffer. The flow time of the buffer alone was measured in a calibrated Cannon-Manning semi-micro viscometer (size 50) after reaching 30 degrees C in a Cannon Instrument Company CT-500 constant temperature waterbath. The viscometer was cleaned and then loaded with the HS DNA sample, allowed to equilibrate in the water bath for 15 minutes, and the flow time was measured. A 2.5 mM sample of the metal complex (MC) was prepared in the dark using the same buffer. A 5 µL aliquot of the metal complex solution was loaded into the viscometer with a long glass rod, mixed, and the flow time was measured. This step was repeated until 25 µL total of metal complex had been added. To plot $(\eta/\eta_0)^{1/3}\ vs.\ [MC]/[DNA]_{bp}$ the changes in relative viscosity were calculated using $\frac{\eta}{\eta_0} = \frac{t - t_0}{t_{DNA} - t_0}$ where t = flow time of DNA solution with the metal complex, t_0= flow time of buffer alone, and t_{DNA} = flow time of DNA solution.

6 Quantum yield of ligand exchange

The quantum yields for CO release were determine in water solution using 470 nm LED irradiation. The decrease in the lowest energy MLCT absorption maximum was monitored as a function of time, and the extinction coefficient and solution volume were used to convert the absorbance values into moles of reactant. A plot of the moles of reactant vs time gives a linear trend considering only early times at which the absorbance changes by < 10%; the slope of this line represents the rate of moles of reactant lost. The photon flux of the LEDs was determined to be $1.19 \times 10^{-8} \pm 7.13 \times 10^{-7}$ mol photons/s using ferrioxalate actinometry as described previously.[2] The quantum yield for CO release was calculated by dividing the rate of moles of reactant lost by the photon flux.

7 List of Figures

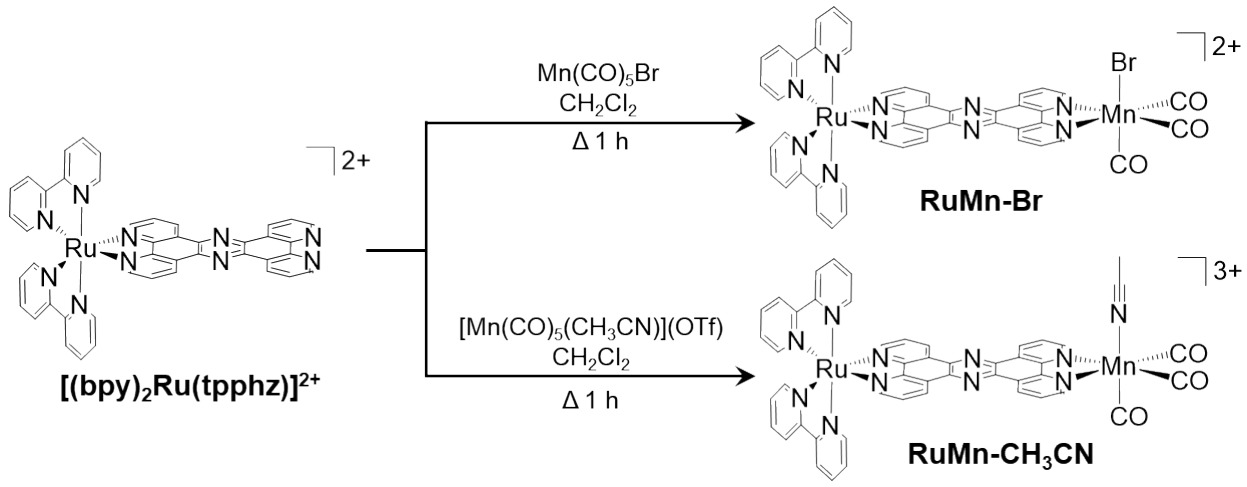

Figure S 1. Synthetic scheme for the preparation of **RuMn-Br** and **RuMn-CH_3CN.**

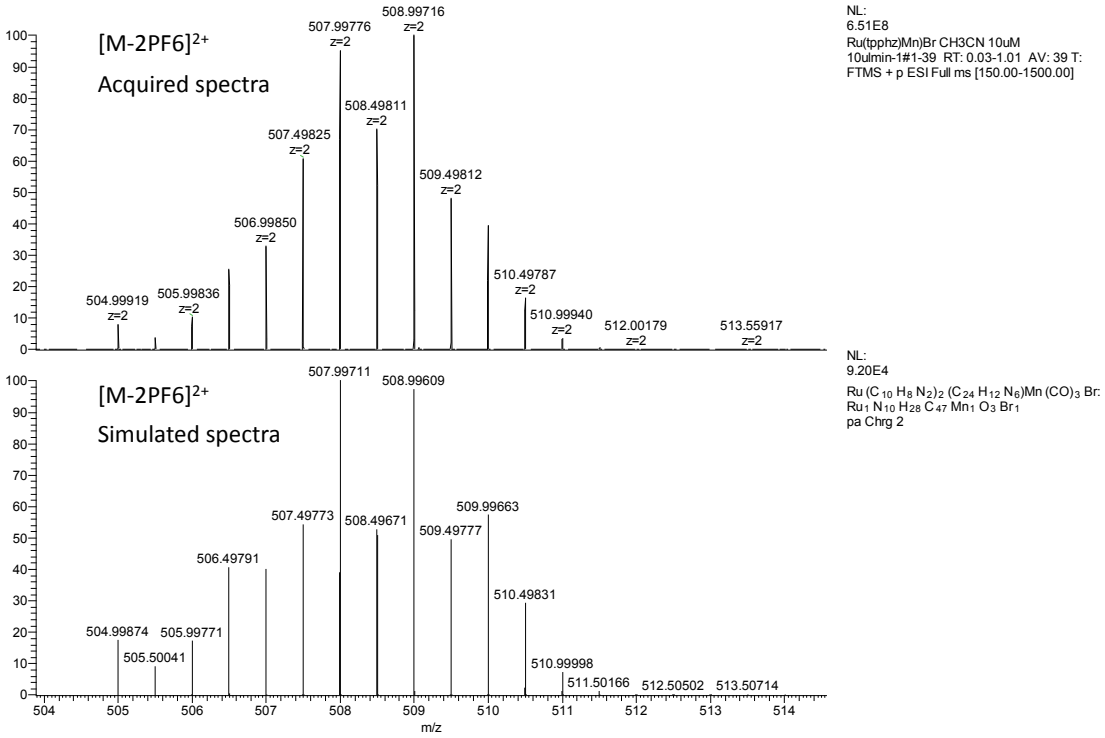

Figure S 2. HR-MS of **RuMn-Br** in CH_3CN and simulated spectrum of **[RuMn-Br -2(PF_6)]$^{2+}$**.

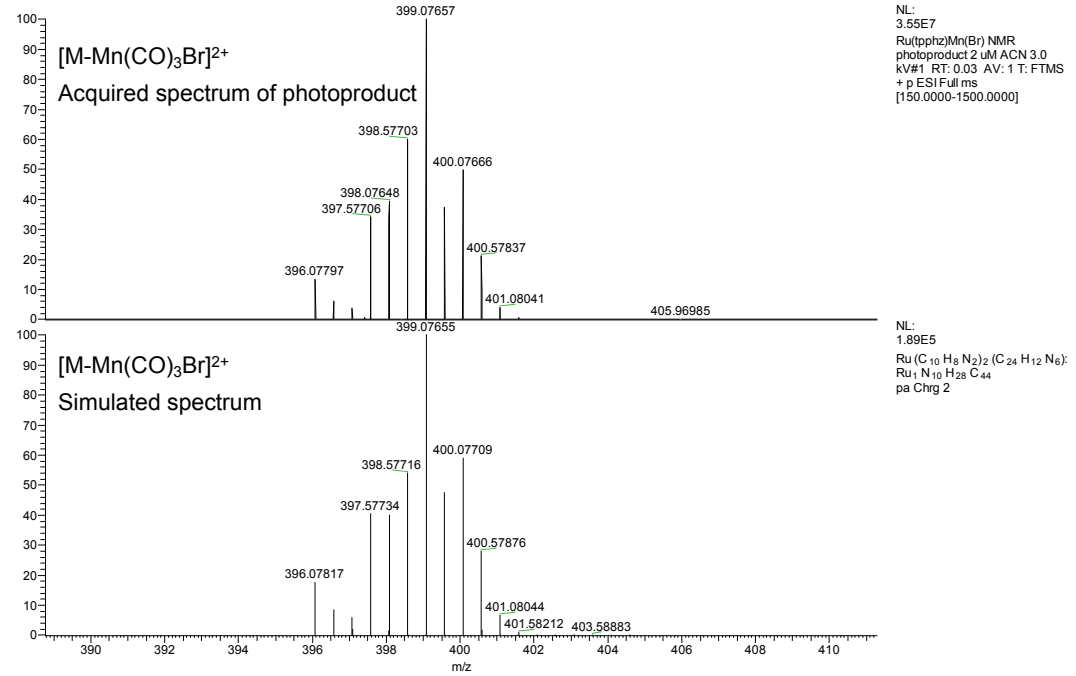

Figure S 3. HR-MS of **RuMn-Br photoproduct** in CH_3CN.

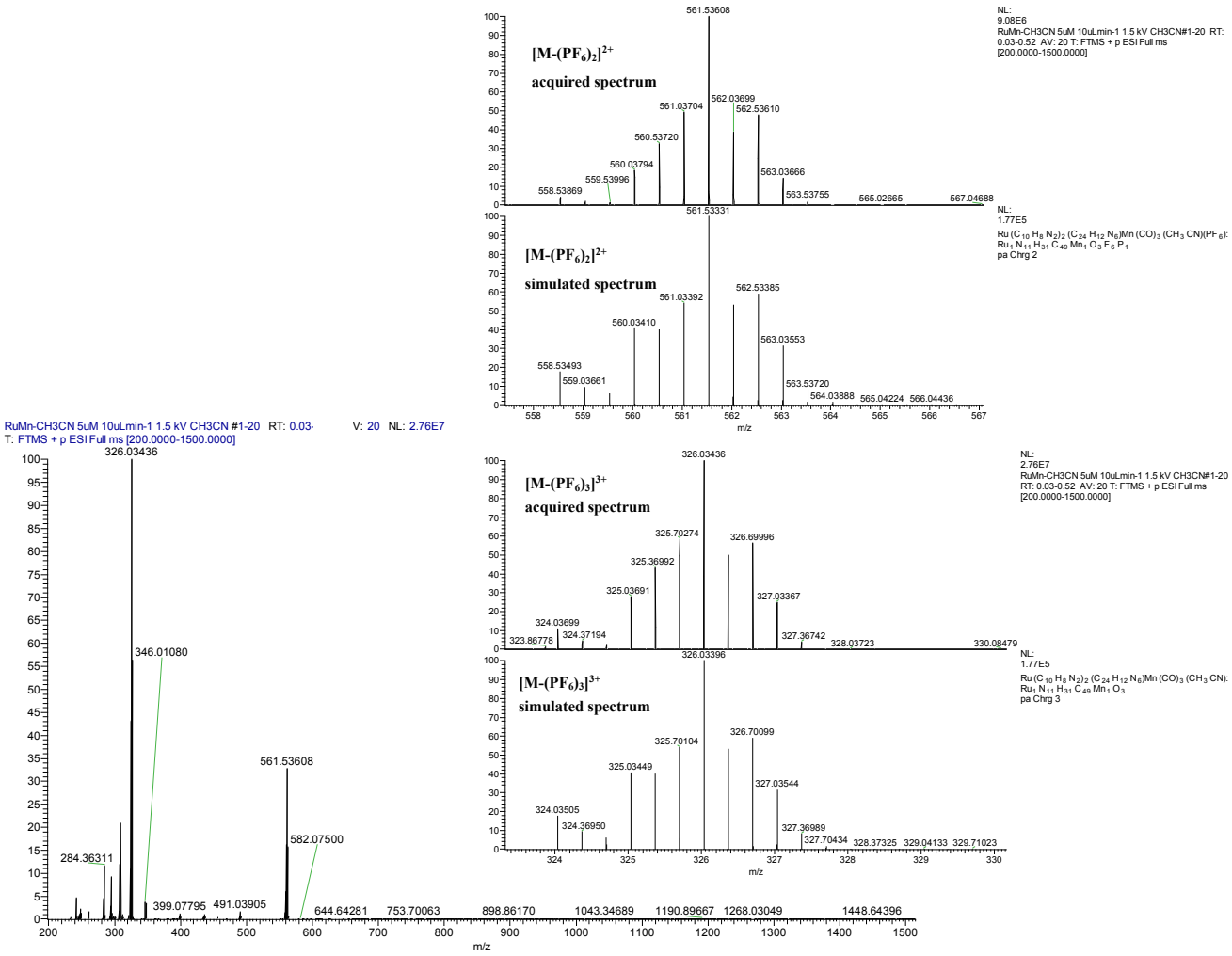

Figure S 4. HR-MS **RuMn-CH$_3$CN** in CH$_3$CN and simulated spectrum of [**RuMn-CH$_3$CN –2(PF$_6$)**]$^{2+}$ and **[RuMn-CH$_3$CN -3(PF$_6$)]$^{3+}$.**

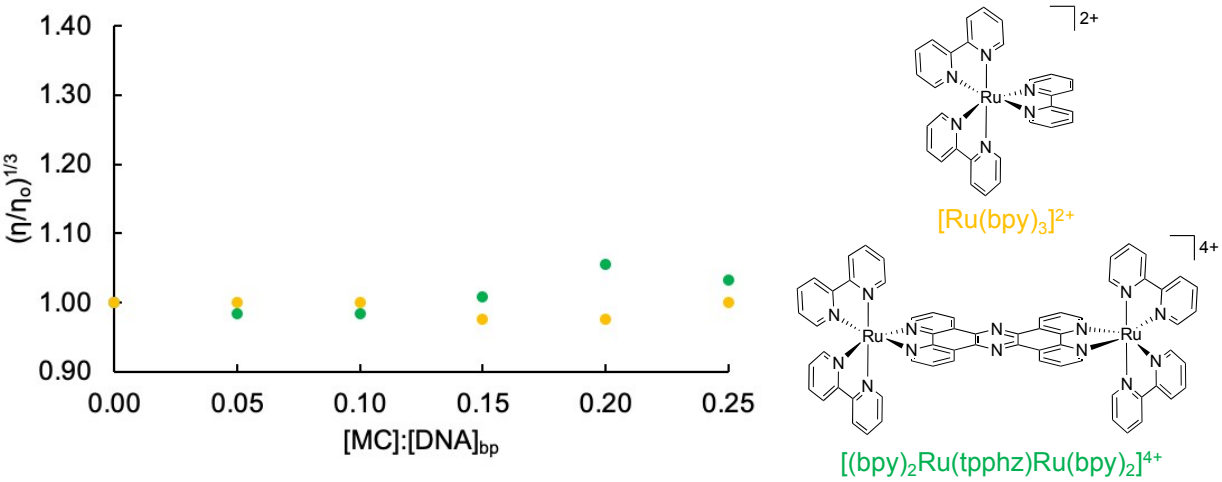

Figure S 5. HS DNA Relative Viscosity $[(bpy)_2Ru(tpphz)Ru(bpy)_2]^{4+}$ (●) and $[Ru(bpy)_3]^{2+}$ (●).

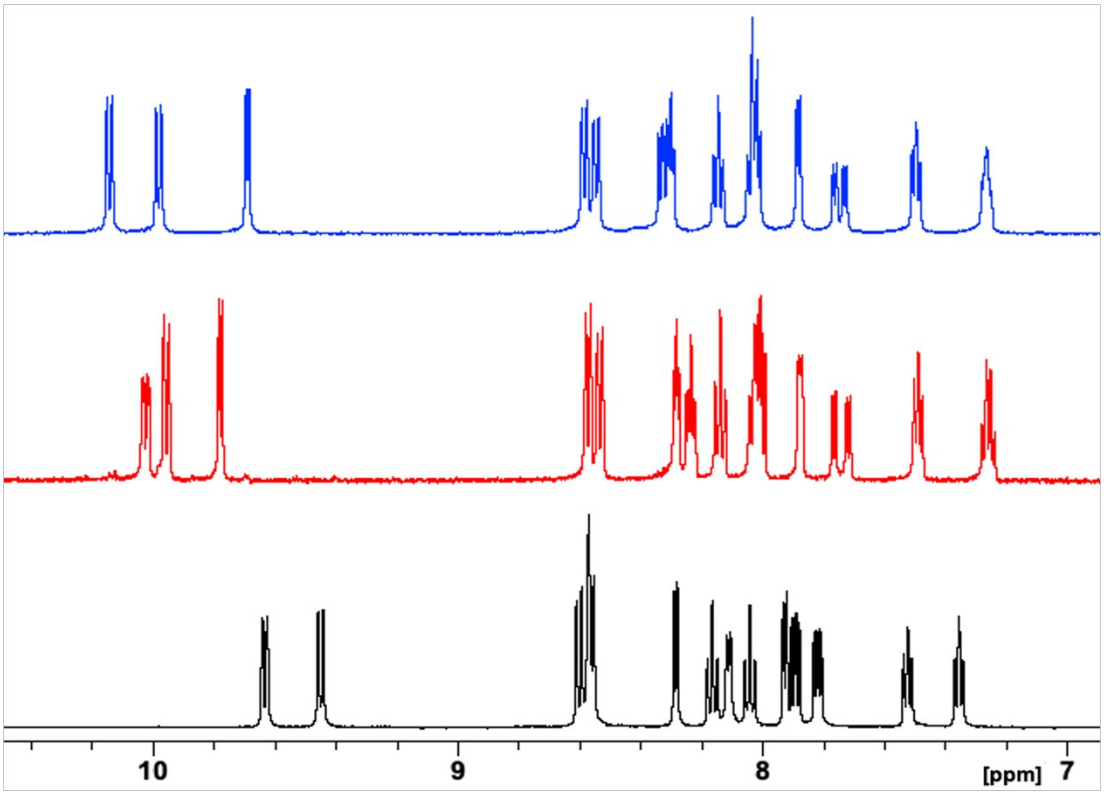

Figure S 6. ^{1}H NMR 5.0 mM in CD_3CN of **Ru(tpphz)** (black), **RuMn-Br** (red), and **RuMn-CH_3CN** (blue).

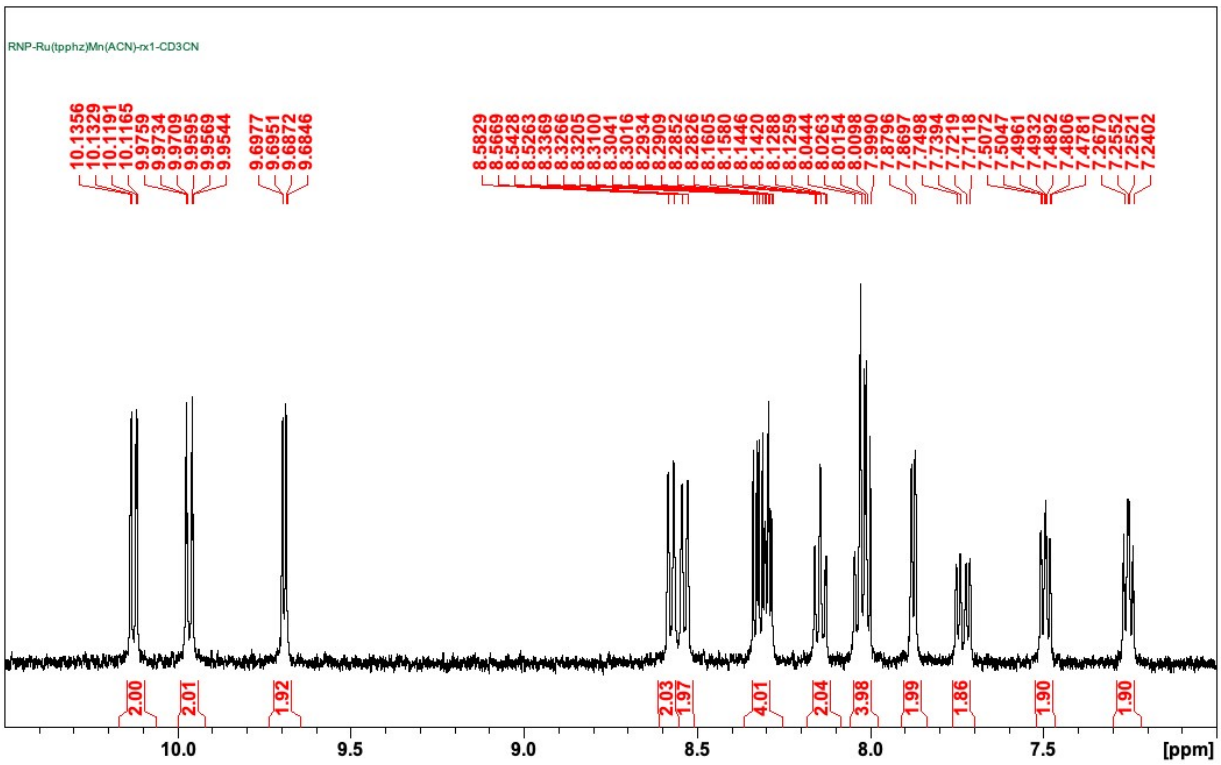

Figure S 7. ^{1}H NMR **RuMn-CH$_3$CN** in CD$_3$CN.

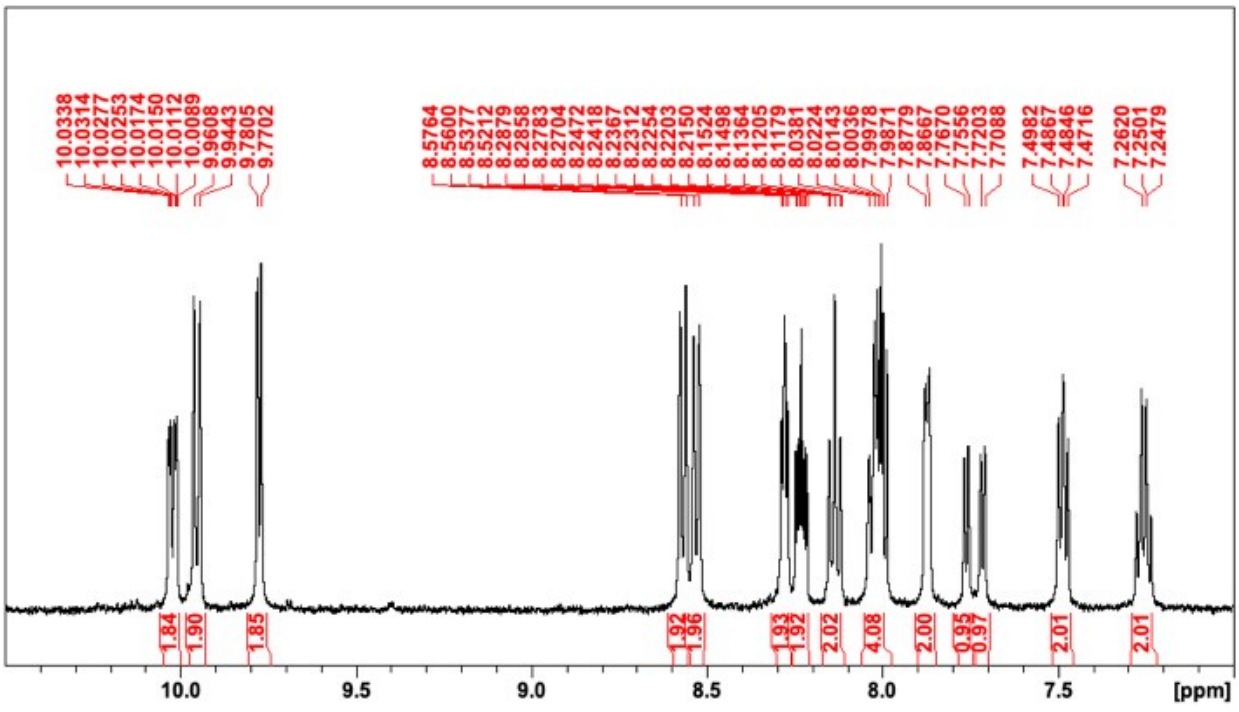

Figure S 8. ^{1}H NMR **RuMn-Br** in CD$_3$CN.

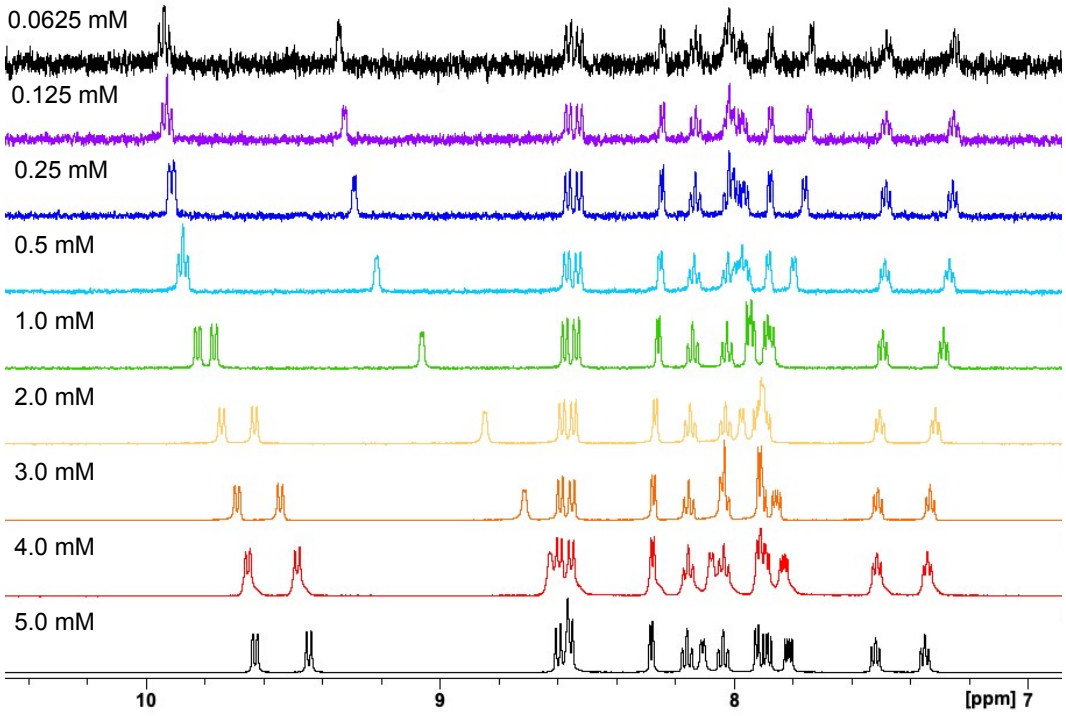

Figure S 9. ^{1}H NMR **Ru(tpphz)** in CD_3CN are varied concentrations.

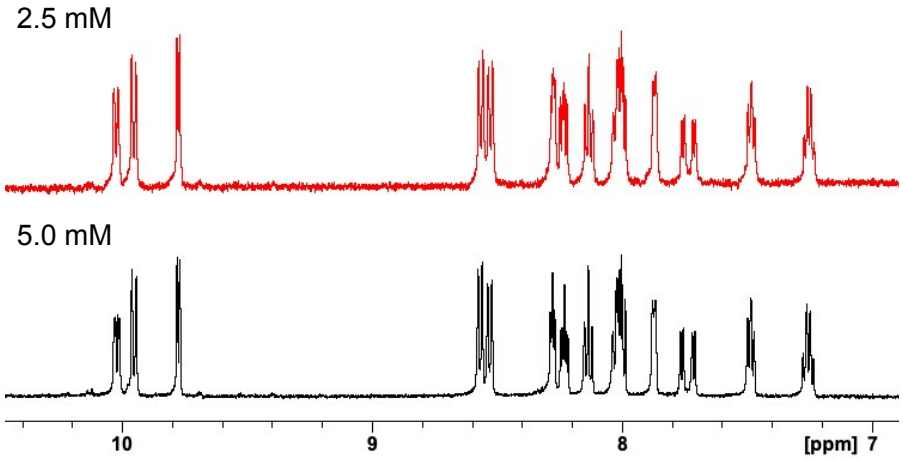

Figure S 10. ^{1}H NMR **RuMn-Br** 5.0 mM (bottom), 2.5 mM (top) in CD_3CN.

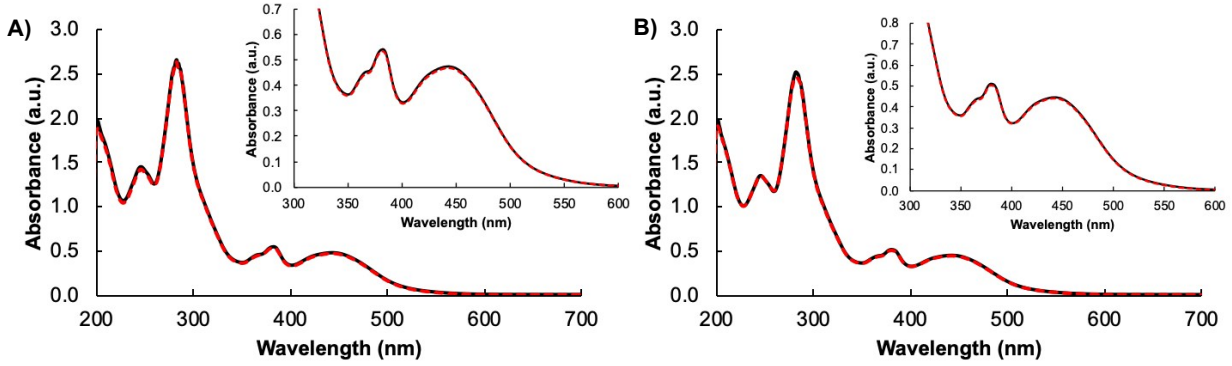

Figure S 12. Dark Controls, initial (solid black) and 18 h (red dash), in rt 5 mM Tris, 50 mM NaCl buffer for **RuMn-CH_3CN** (A) and **RuMn-Br** (B).

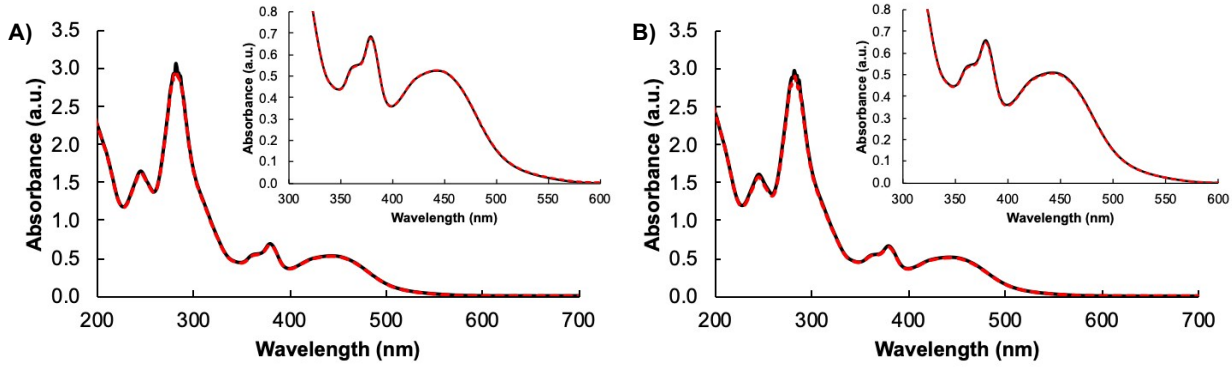

Figure S 11. Dark Controls, initial (solid black) and 18 h (red dash), in rt water for **RuMn-CH_3CN** (A) and **RuMn-Br** (B).

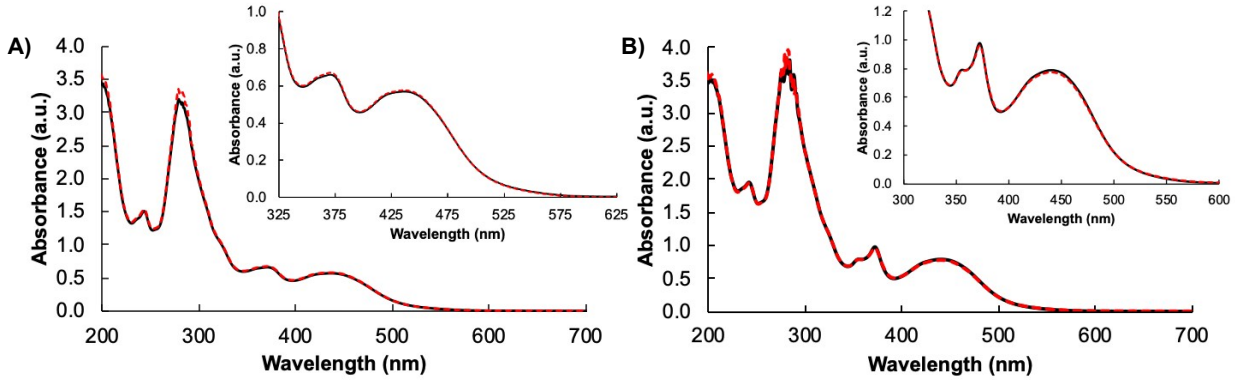

Figure S 13. Dark Controls, initial (solid black) and 1 h (red dash), in rt CH_3CN for **RuMn-CH_3CN** (A) and **RuMn-Br** (B).

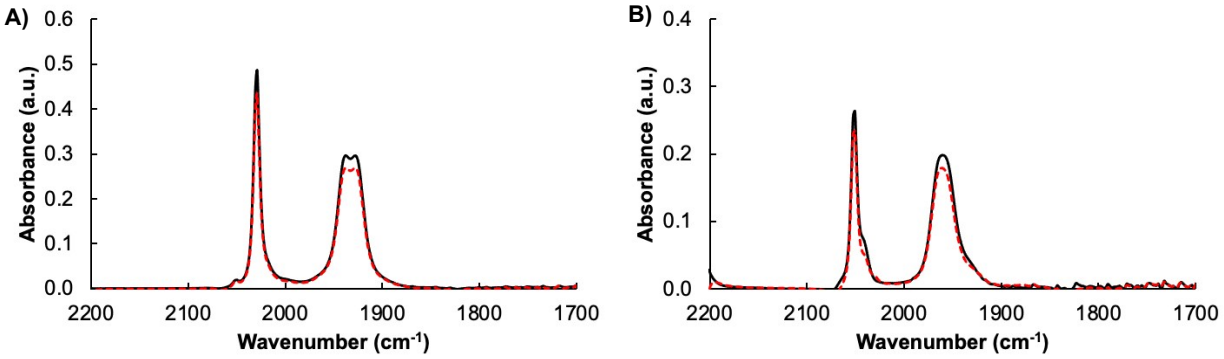

Figure S 14. FTIR dark control of **RuMn-Br** (A) and **RuMn-CH_3CN** (B) in rt CH_3CN 0 h (black) and 1 h (red dash).

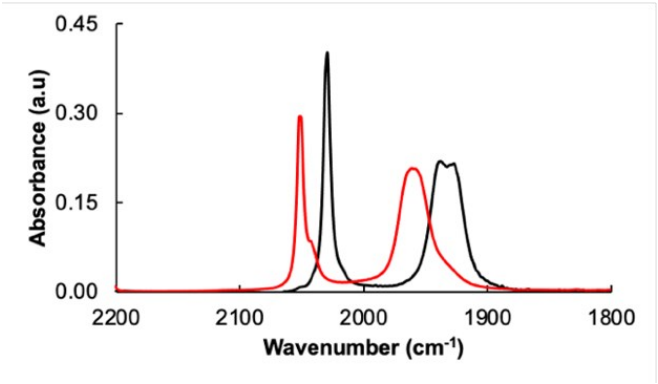

Figure S 15. FTIR spectra for **RuMn-Br** (black) and RuMn-CH_3CN (red) in rt CH_3CN (1 mM) in the dark.

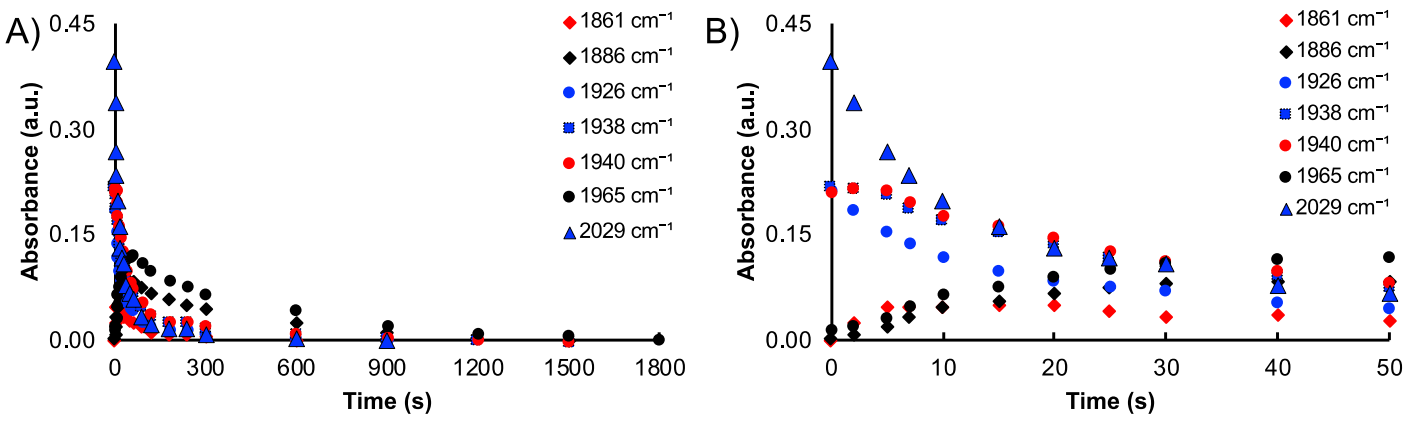

Figure S 16. FTIR absorbance values versus irradiation time of **RuMn-Br** with wavenumbers of initial complex (blue), the first observable intermediate (red), and second observable intermediate (black) (A) Initial irradiation times (B).

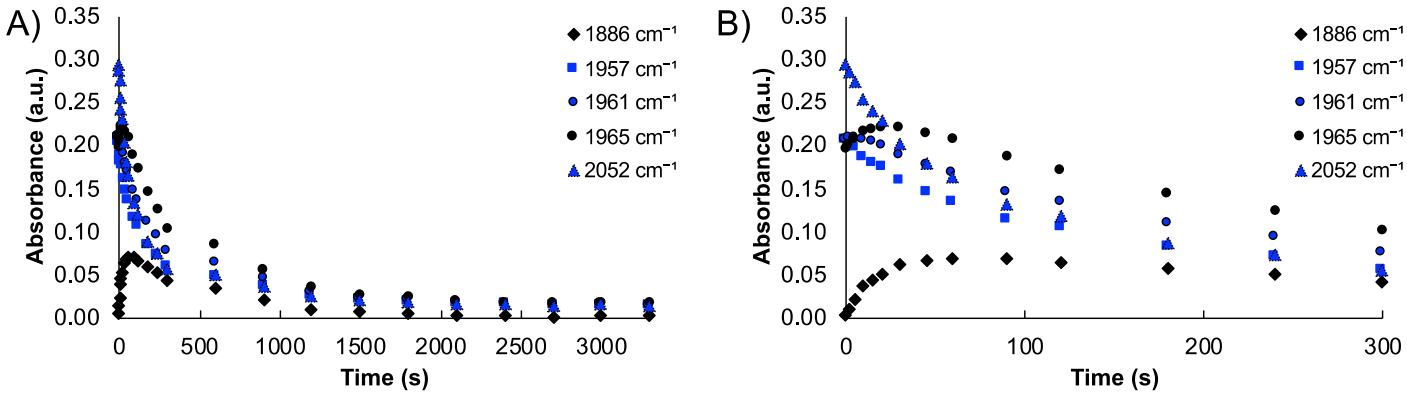

Figure S 17. FTIR absorbance values versus irradiation time of **RuMn-CH_3CN** with wavenumbers of initial complex (blue), and the first observable intermediate (black) (A) Initial irradiation times (B).

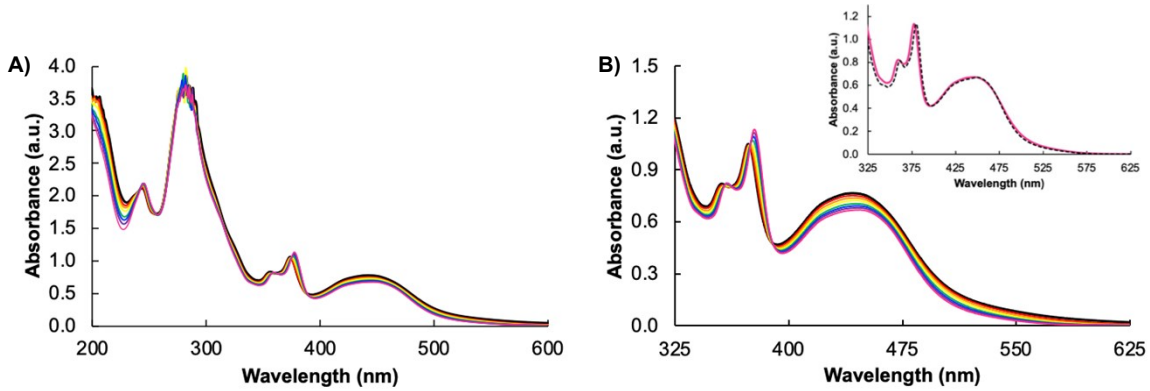

Figure S 18. Absorbance measurements of **RuMn-Br** 470 nm photolysis in rt CH_3CN 0 - 15 min (A) Limited spectral view of 470 nm photolysis of **RuMn-Br** in rt CH_3CN with inset showing overlay of **RuMn-Br photoproduct** with **Ru(tpphz)** in CH_3CN (B).

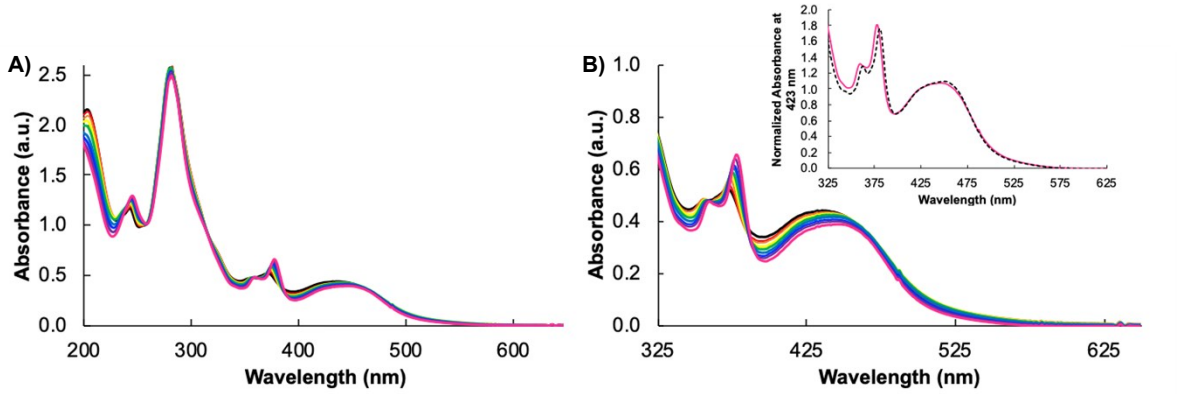

Figure S 19. Absorbance measurements of **RuMn-CH_3CN** 470 nm photolysis in rt CH_3CN 0 - 30 min (A) Limited spectral view of 470 nm photolysis of **RuMn-CH_3CN** in rt CH_3CN with inset showing overlay of **RuMn-CH_3CN photoproduct** with **Ru(tpphz)** in CH_3CN (B).

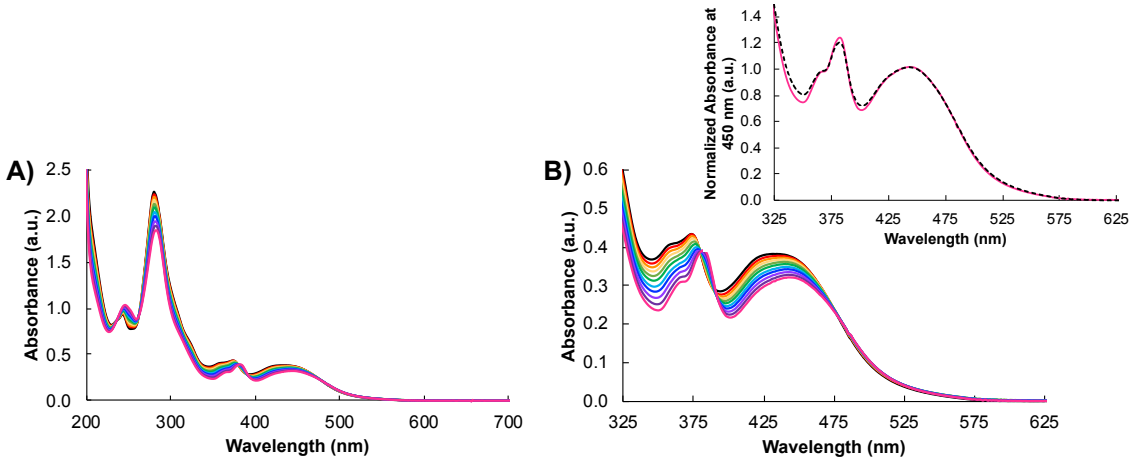

Figure S 20. Absorbance measurements of **RuMn-CH_3CN** 470 nm photolysis in rt 5 mM Tris 50 mM NaCl buffer 0 - 40 min (A) Limited spectral view of 470 nm photolysis of **RuMn-CH_3CN** in rt 5 mM Tris 50 mM NaCl buffer with inset showing overlay of **RuMn-CH_3CN photoproduct** with **Ru(tpphz)** in 5 mM Tris 50 mM NaCl buffer (B).

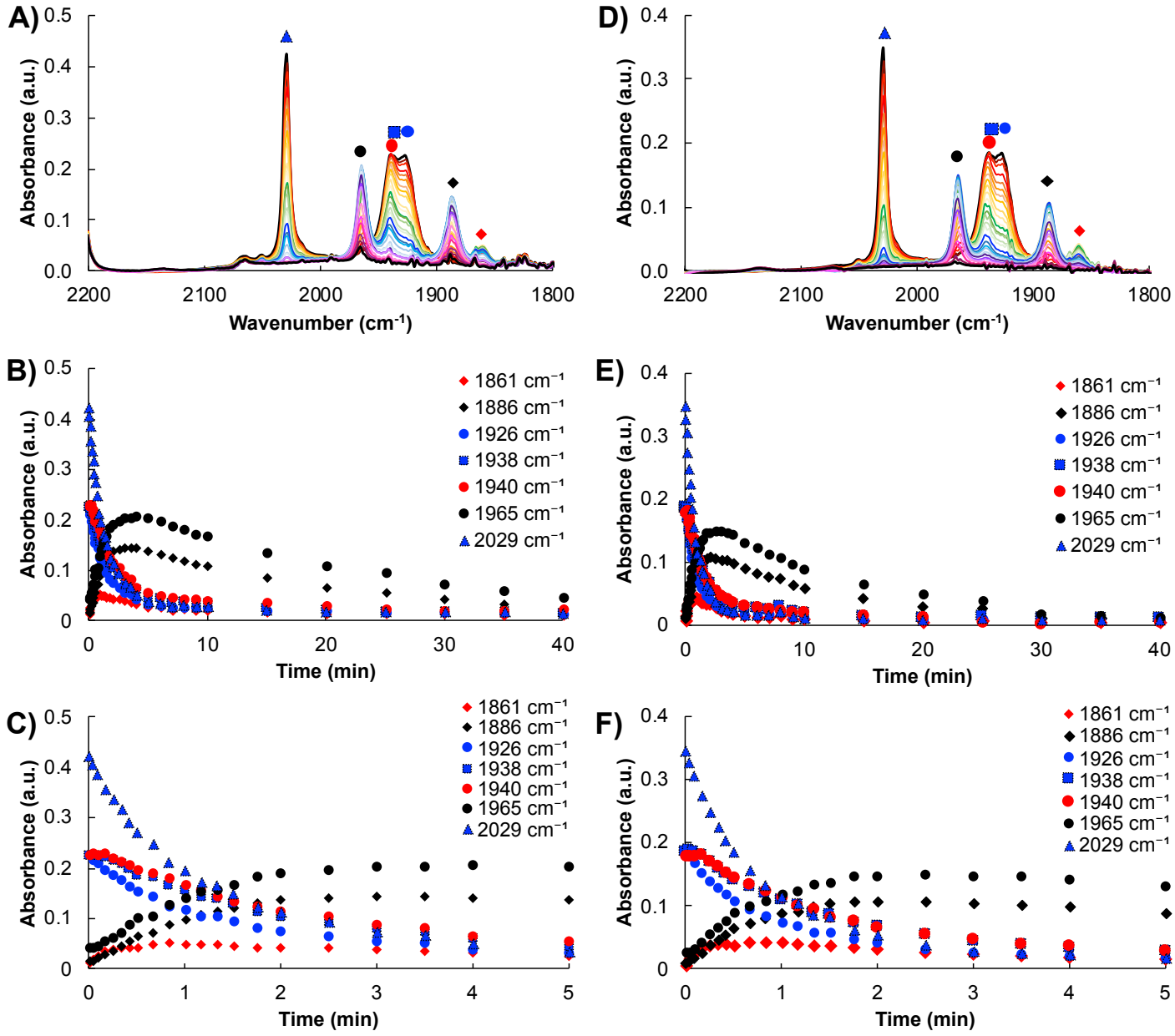

Figure S 21. FTIR absorbance values versus irradiation time of **RuMn-Br** in degassed CH_3CN **(A-C)** aerated CH_3CN **(D-F)** with wavenumbers of initial complex (blue), the first observable intermediate (red), and second observable intermediate (black) **(B and E)** Initial irradiation times **(C and F)**.

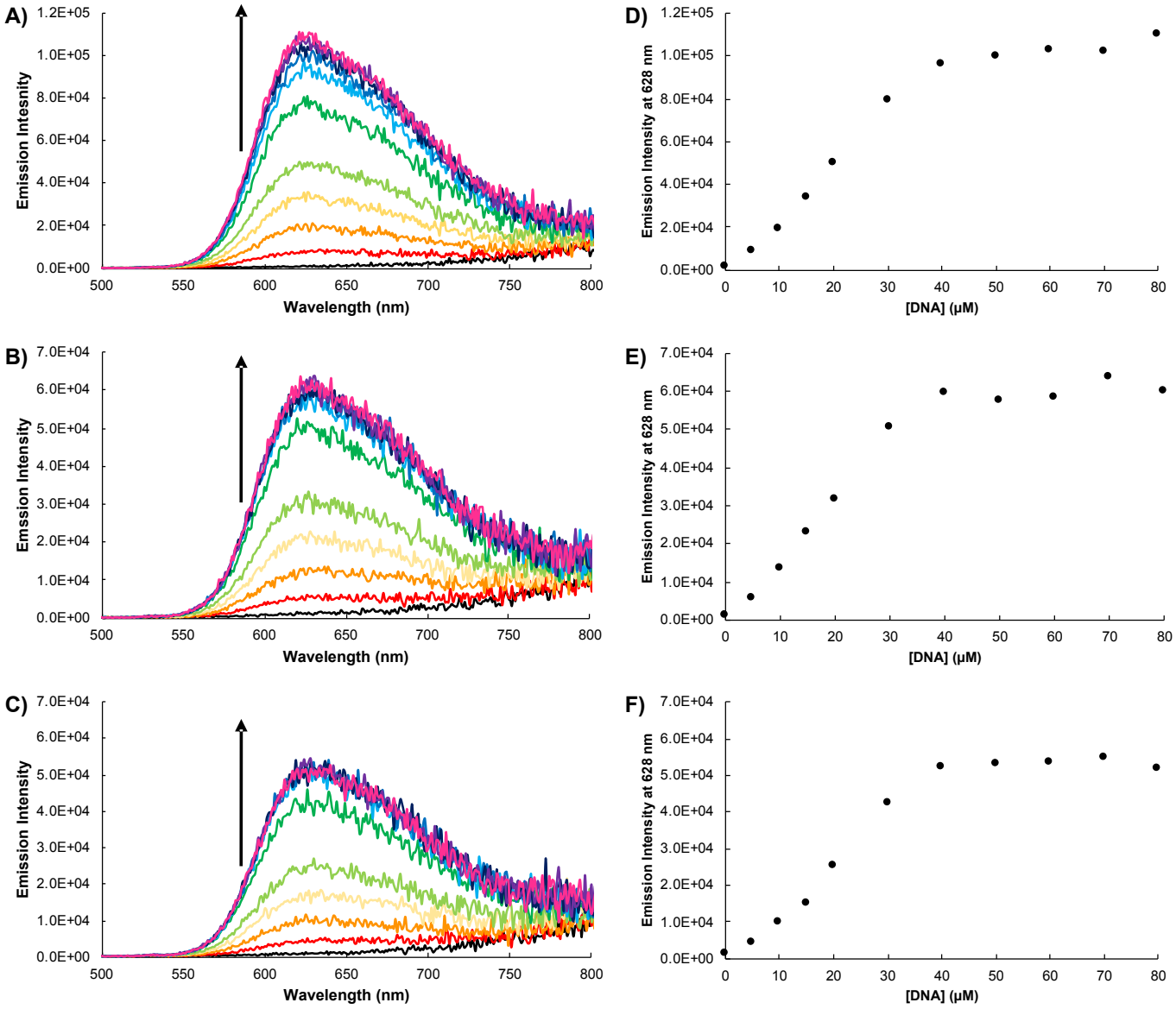

Figure S 22. Emission spectra of **Ru(tpphz) (A) RuMn-Br photoproduct (B)** and **RuMn-CH_3CN photoproduct (C)** 7.5 μM in buffer (5 mM Tris, 50 mM NaCl, pH= 7.5) at room temperature with increasing [CT-DNA] up to 80 μM. λ_{ex}= 450 nm. A plot of increasing emission intensity at 628 nm as a function of increasing [CT-DNA] for **Ru(tpphz) (D) RuMn-Br photoproduct (E)** and **RuMn-CH_3CN photoproduct (F)**.

8 References

1 J. Bolger, A. Gourdon, E. Ishow and J.-P. Launay, Inorg. Chem., 1996, 35, 2937–2944.

2 Montalti, M.; Credi, A.; Prodi, L.; Gandolfi, M. T., *Handbook of Photochemistry*. CRC press: 2006.